Power Management of Virtual Synchronous Generators through using Hybrid Energy Storage Systems

Jingyang Fang, Xiaoqiang Li, Yi Tang
School of Electrical and Electronic Engineering
Nanyang Technological University
Singapore
E-mail: jfang006@e.ntu.edu.sg, lixiaoqiang@ntu.edu.sg, yitang@ntu.edu.sg

Hongchang, Li
Energy Research Institute @ NTU (ERI@N)
Nanyang Technological University
Singapore
E-mail: hongchangli@ntu.edu.sg

***Abstract*— The increasing demand for clean energy necessitates a large-scale integration of renewable energy sources (RESs), which has dramatically changed the paradigm of modern power systems. Conventionally, synchronous generators with rotating reserves are responsible for system frequency regulation. As the penetration of RESs grows, the task of frequency regulation is supposed to be gradually taken over by virtual synchronous generators (VSGs), which are essentially grid-interfaced power converters behaving similarly to synchronous generators. Nonetheless, unlike synchronous generators, VSGs do not possess spinning reserves, and hence, energy storage systems (ESSs) are required in VSGs. However, the implementation and coordination control of ESSs in VSGs have not been investigated. To fill this research gap, this paper proposes a hybrid ESS (HESS) consisting of a battery and an ultracapacitor to achieve the power management of VSGs. During load disturbances, the ultracapacitor tackles the fast-varying power introduced by inertia emulation while the battery implements the remaining parts of VSGs and only compensates for relative long-term power fluctuations with slow dynamics. In this way, the proposed HESS allows reduction of the battery power fluctuations along with its changing rate. Finally, experimental results are presented to illustrate the effectiveness of the proposed concept.**

Keywords—Energy storage system (ESS); frequency regulation; renewable energy source (RES); virtual synchronous generator (VSG)

I. INTRODUCTION

The increasing penetration of renewable energy sources (RESs) has changed the paradigm of modern power systems [1]. Nowadays, synchronous generators are responsible for frequency regulation. When frequency events occur, they perform inertial response, which can slow down the frequency dynamics by absorbing or delivering the kinetic energy stored in the rotors of synchronous generators and turbines [2]. In the future, the task of frequency regulation will be taken over by grid-connected power converters. At present, most of the grid-connected power converters are operated to extract the maximum power from RESs without providing any frequency regulation capability [3, 4].

An emerging concept for power converters to implement frequency regulation is known as virtual synchronous generators (VSGs) or virtual synchronous machines (VSMs) [5−7]. The basic idea behind this concept lies in the emulation of synchronous generators. However, previous research works only concentrate on VSG control and rarely discuss the practical implementation of VSGs. In [8−10], the VSG is simply implemented as an inverter fed by an ideal DC power supply. All the control loops in the VSG, e.g. inertia and speed governor, are realized by the ideal DC voltage source, which is obviously not the real case. In fact, energy storage systems (ESSs) must be involved in VSGs to achieve frequency regulation, and the implementation and coordination control of ESSs in VSGs have not been investigated in the literature.

For selection of energy storage units in an ESS, it would be desirable that high energy density units and high power density units are used together so as to increase the system operating efficiency and/or lifetime as well as reduce system costs. One example is the hybrid ESS (HESS) composed of a battery and an ultracapacitor, where the battery is used for compensation of low frequency power fluctuations and the ultracapacitor is used for compensation of high frequency power fluctuations [11−15]. To fully exploit the advantages of different energy storage units, low/high pass filters are normally employed to extract low/high frequency power fluctuations in the system. However, there is no guideline on how to design the cut-off frequency of such filters and it is typically determined through trial and error [13-15].

In view of the aforementioned issues, a battery/ultracapacitor HESS applied to VSGs is proposed in this paper. Specifically, the ultracapacitor is used to emulate the inertia of a VSG, as this part of the VSG is designed to cope with high frequency power fluctuations. The remaining parts of the VSG, e.g. droop control and turbine model, are emulated by the battery, as they are tasked at compensating for relatively long-term power fluctuations with slow dynamics. In this way, one can fully utilize the advantages of the ultracapacitor and battery to realize a practical VSG system.

978-1-5386-1180-7/18/$31.00 ©2018 IEEE

The power references of the ultracapacitor and battery are respectively derived from the virtual inertia emulation and the remaining parts of the VSG control rather than conventional low/high pass filters. Moreover, since the HESS is used to emulate frequency regulation implemented by conventional frequency regulators, the control parameters for the HESS can easily be designed based on the VSG model.

II. System Description

Conventionally, the VSG system is simply implemented by an ideal DC voltage source connected to an inverter. By controlling the inverter to mimic the operation of synchronous generators, the objective of frequency regulation can be achieved [8−10]. However, the ESS included in the VSG system is always neglected. In contrast, Fig. 1 illustrates the schematic diagram of the proposed system, where f_g denotes the system frequency, f_o, ω_o, and θ_o represent the output frequency, angular frequency, and phase-angle, and the PLL stands for the abbreviation of the phase-locked-loop. In Fig. 1, frequency regulation is implemented by a battery/ultracapacitor HESS. This HESS can be implemented with various architectures, as it can be visualized from Fig. 2. Fig. 2(a) presents the simplest architecture, where the two units are directly connected in parallel. In this case, the independent power control cannot be achieved. As compared with Fig. 2(b), Fig. 2(c) allows to reduce the voltage rating of the battery. Although Figs. 2(d) and (e) enable flexible power controls, an additional DC/DC power converter is required. Considering the system controllability and simplicity, the architecture shown in Fig. 2(c) is eventually employed in this paper. In this case, the battery is connected to the ultracapacitor through a DC/DC converter, and an *LC*-filtered three-phase inverter is employed as the interface between the ultracapacitor and AC load.

In Fig. 1, the voltage controller is dictated to follow the voltage references given by the frequency controller. Fig. 3 shows the control block diagrams of the voltage controller, where the subscripts *ref* and *pu* stand for the reference value and per-unit value and Δ denotes the change of relevant parameters. Note that the voltage controller consists of two separate parts for regulating the DC/DC converter and inverter, respectively. The DC/DC voltage controller performs the regulation of the DC-link voltage v_{dc} while the three-phase AC output voltages v_{ci} ($i = a, b, c$) are regulated in the synchronous *dq* frame by the inverter voltage controller. Both controllers are constructed following the standard cascaded control structure, which includes an inner current-loop and an outer voltage-loop [16].

The detailed control block diagram of the frequency controller is illustrated in Fig. 4, where P_{in_pu} stands for the input power of the VSG, P_{l_pu} signifies the frequency-independent load power, R_d denotes the droop-coefficient, D represents the damping factor of the frequency-dependent loads, and H designates the combined inertia coefficient, which is defined as the ratio of the rotational kinetic energy stored in the rotors of synchronous generators to the system base power. This frequency controller functions similarly to the standard frequency regulator of synchronous generators, which can be found from page 598 to page 601 in [2]. The dynamics of the speed governor and reheat turbine are also included in Fig. 4.

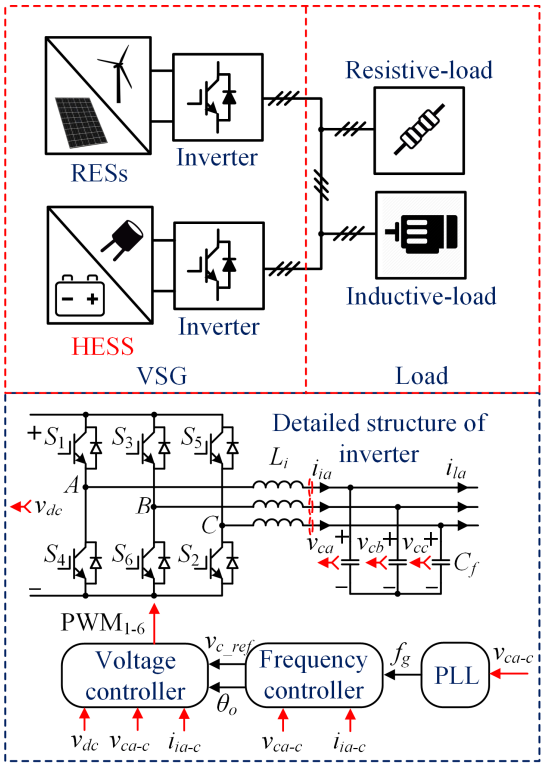

Fig. 1. Schematic diagram of the VSG system.

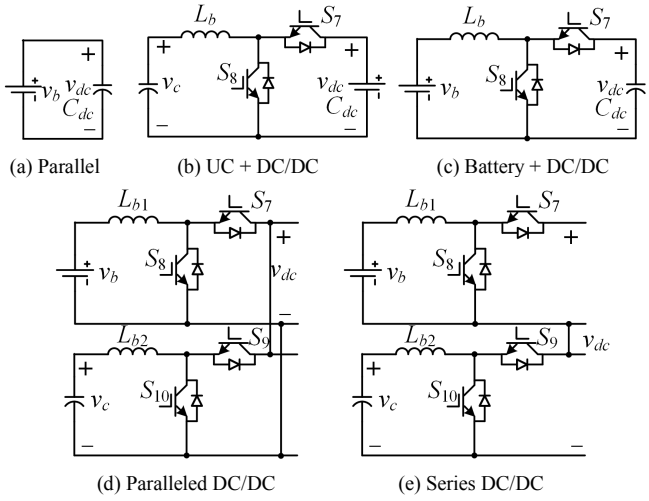

Fig. 2. Architectures of the HESS.

The most important feature of the proposed controllers is highlighted in Fig. 3(a). As observed, the DC-link voltage reference $\Delta v_{cdc\_ref\_pu}$ is dynamically adjusted according to the system frequency deviation Δf_{g_pu} through a gain K_f. With this method, the power allocation between the battery and ultracapacitor can be achieved and will be explained in the next section.

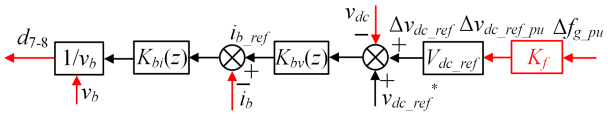

(a) DC/DC converter

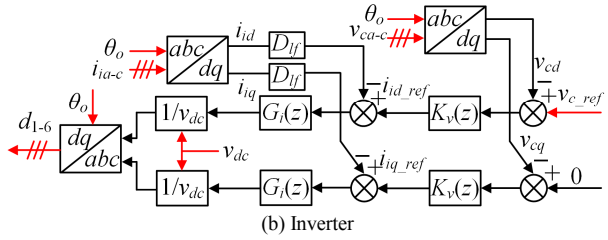

(b) Inverter

Fig. 3. Structures of the voltage controller.

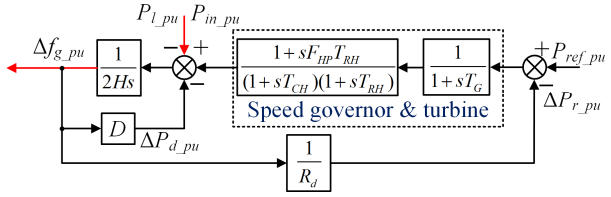

Fig. 4. Structure of the frequency controller.

III. Power Management Scheme

Since frequency regulation is mainly determined by active power, the control blocks concerning reactive power are ignored here. From Fig. 4, the following well-known swing equation can be obtained [2]:

$$\Delta P_{in\_pu} - \Delta P_{l\_pu} = D\Delta f_{g\_pu} + 2H\frac{d\Delta f_{g\_pu}}{dt}, \tag{1}$$

or

$$\Delta P_{l\_pu} + \Delta P_{d\_pu} = \underbrace{\Delta P_{in\_pu}}_{\text{Battery}} + \underbrace{\left(-2H\frac{d\Delta f_{g\_pu}}{dt}\right)}_{\text{Ultracapacitor}}, \tag{2}$$

where ΔP_{l_pu} is the power variation caused by loads and RESs and $\Delta P_{d\_pu} = D\Delta f_{g\_pu}$ is the power variation caused by the frequency-dependent loads. ($\Delta P_{in\_pu} - 2Hd\Delta f_{g\_pu}/dt$) is the power change of the VSG used for balancing the load and RES power variations in real time. As shown in Fig. 4, ΔP_{in_pu} should follow the power reference given by the frequency-droop $-\Delta P_{r\_pu}$, and it changes slowly due to the time delay introduced by the speed governor and turbine. ΔP_{in_pu} equals $-\Delta f_{g\_pu}/R_d$ in the steady-state. $-2Hd\Delta f_{g\_pu}/dt$ is the VSG power contributed by inertia emulation. This term varies very fast as it is in proportion to the time derivative of frequency.

Fig. 5 visualizes the principle of the proposed power management scheme. The fundamental idea behind the proposed power management scheme is to allocate fast-varying $-2Hd\Delta f_{g\_pu}/dt$ to the ultracapacitor and the slowly-changing ΔP_{in_pu} to the battery so that the advantages of these energy storage units can fully be utilized. The following equations should be satisfied to achieve this objective,

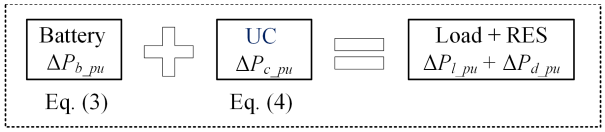

Fig. 5. Principle of the proposed power management scheme.

$$\Delta P_{b\_pu} = \Delta P_{in\_pu} = -\frac{\Delta f_{g\_pu}}{R_d} * K_p(t), \tag{3}$$

$$\Delta P_{c\_pu} = -2H\frac{d\Delta f_{g\_pu}}{dt}, \tag{4}$$

where "*" stands for the convolution operation, $K_p(t)$ denotes the time-domain model of the speed governor and turbine, ΔP_{b_pu} and ΔP_{c_pu} respectively represent the power changes of the battery and ultracapacitor. ΔP_{c_pu} can alternatively be expressed as the following equation by differentiating the energy stored in the ultracapacitor:

$$\begin{aligned}\Delta P_{c\_pu} &= -\frac{1}{P_{ref}}\cdot\frac{d[0.5C_{dc}(V_{dc\_ref}+\Delta v_{dc})^2]}{dt}\\ &= -\frac{C_{dc}V_{dc\_ref}}{P_{ref}}\cdot\frac{d\Delta v_{dc}}{dt} = -\frac{C_{dc}V_{dc\_ref}^{\ 2}}{P_{ref}}\cdot\frac{d\Delta v_{dc\_pu}}{dt}\\ &= -2H_c\frac{d\Delta v_{dc\_pu}}{dt}\end{aligned} \tag{5}$$

where $H_c = 0.5C_{dc}V_{dc\_ref}^{\ 2}/P_{ref}$ represents the inertia coefficient of the ultracapacitor, P_{ref} stands for the system rated/base power used for normalization, and the capacitor voltage deviation is also normalized by $\Delta v_{dc} = V_{dc\_ref}\Delta v_{dc\_pu}$. Since Δv_{dc_pu} is related to Δf_{g_pu} with $\Delta v_{dc\_pu} = K_{fv}\Delta f_{g\_pu}$ as defined by the frequency controller shown in Fig. 3(a), ΔP_{c_pu} can be expressed as:

$$\begin{aligned}\Delta P_{c\_pu} &= -2H_c\frac{d\Delta v_{dc\_pu}}{dt} = -2K_{fv}H_c\frac{d\Delta f_{g\_pu}}{dt}\\ &= -2H\frac{d\Delta f_{g\_pu}}{dt} \Rightarrow H = K_{fv}H_c.\end{aligned} \tag{6}$$

From (6), the desired proportional gain K_{fv} can be derived as:

$$K_{fv} = \frac{2HP_{ref}}{C_{dc}V_{dc\_ref}^{\ 2}}. \tag{7}$$

It should be noted that the maximum value of K_{fv} depends on the allowable deviations of the DC-link voltage and system frequency [17]. To ensure linear modulation and avoid overstresses of semiconductors, a less than 15% DC-link voltage deviation is desired. Based on the above analysis, the control parameter values can be derived from the system parameter values and listed in Table I, where the emulated power system inertia H is designed to be 5.0 s, which is similar to the inertia constant of a conventional power system [2].

IV. Experimental Verification

Experiments were carried out based on the system schematic diagram shown in Fig. 1. A photo of the experimental test-bed is shown in Fig. 6. The control

Table I. System and control parameter values.

Description	System parameter		Description	Control parameter	
	Symbol	Value		Symbol	Value
Battery voltage reference	V_{b_ref}	250 V	**Frequency-droop coefficient**	R_d	0.05
DC filter inductance	L_b	5.6 mH	**Speed governor coefficient**	T_G	0.1 s
DC-link voltage reference	V_{dc_ref}	400 V	**Turbine HP coefficient**	F_{HP}	0.3 s
DC-link capacitance	C_{dc}	3.76 mF	**Time constant of reheater**	T_{RH}	7.0 s
AC filter inductance	L_i	1 mH	**Time constant of main inlet**	T_{CH}	0.2 s
AC filter capacitance	C_f	50 µF	**Inertia coefficient**	H	5.0 s
Frequency reference	f_{g_ref}	50 Hz	**Load damping coefficient**	D	1.0
Maximum frequency deviation	Δf_{g_max}	0.2 Hz	**UC inertia coefficient**	H_c	0.3 s
Maximum DC-link voltage deviation	Δv_{dc_max}	27 V	**Frequency-voltage gain**	K_{fv}	16.6
Active power reference	P_{ref}	1 kW	**Gird voltage reference**	V_{c_ref}	110 V rms

algorithms were executed on a dSPACE controller (Microlabbox), and an eight-channel oscilloscope (TELEDYNE LECROY: HDO8038) was used to capture the experimental waveforms.

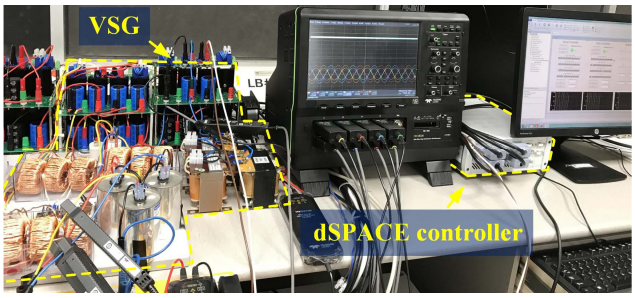

Fig. 6. A photo of the experimental prototype.

Fig. 7 presents the steady-state experimental results of the proposed VSG system. As expected, the waveforms of the AC voltages v_{ci} ($i = a, b, c$) are controlled as clean sinusoidal while the DC-link voltage v_{dc} is maintained as a constant 400 V, thereby proving the effectiveness of voltage control.

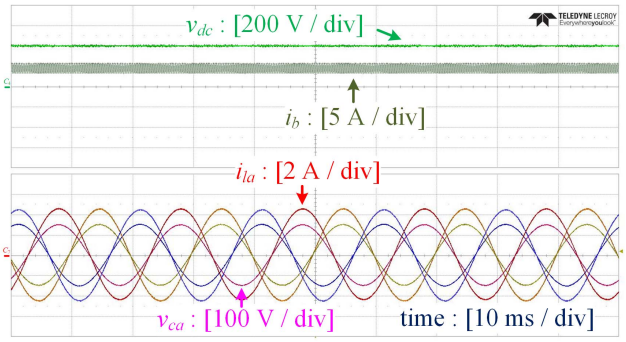

Fig. 7. Steady-state experimental waveforms of the proposed VSG system.

Fig. 8 illustrates the system frequency response under a 3% step-up load change. It can clearly be observed that the VSG exhibits similar inertial frequency response as conventional synchronous generators under this frequency event. Moreover, the DC-link voltage v_{dc} tightly tracks its reference and varies in proportion to the system frequency f_g. As mentioned, the variation of v_{dc} achieves the delivery of the inertial power. As a result, only the slowly-changing power is handled by the battery.

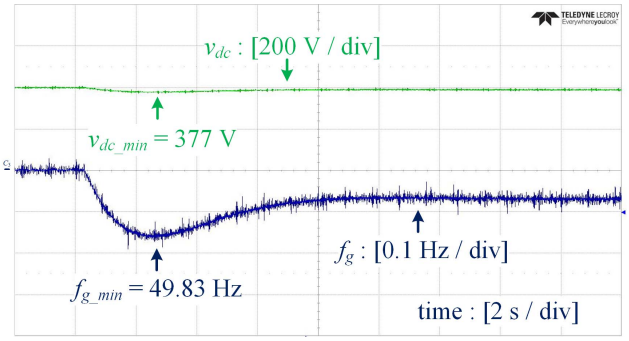

Fig. 8. System frequency responses under a 3% step-up load change.

The effectiveness of the proposed power management scheme is validated by Fig. 9, where the power allocation between the ultracapacitor and battery under the same 3% step-up load change is illustrated. As seen, the ultracapacitor responds promptly to the frequency event, which allows smooth discharge of the battery.

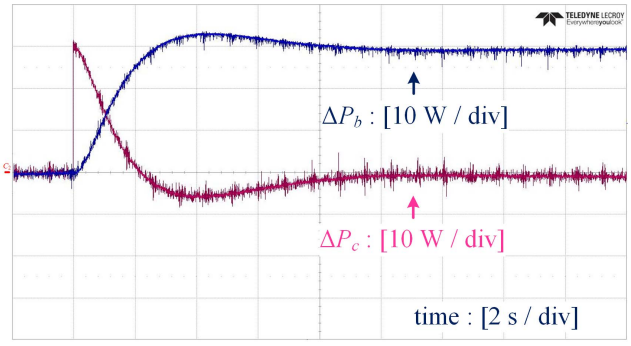

Fig. 9. System power responses under a 3% step-up load change.

Fig. 10 further demonstrates the performance of the HESS under an intermittent RES output, where the power data was

randomly generated to validate the power allocation of the proposed HESS-based VSG. A ramp rate limit of ±10% per second was applied when generating the data set according to [18].

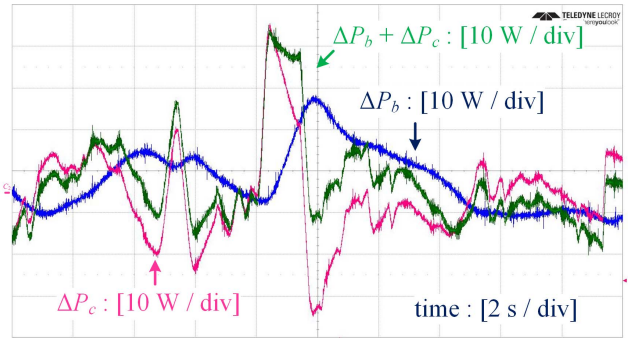

Fig. 10. System power responses under a 3% step-up load change.

Under this scenario, the high frequency power disturbances can again be compensated by the ultracapacitor, and the power fluctuations of the battery can be reduced, which is in consistence with the theoretical analysis.

V. Conclusion

This paper has proposed a battery/ultracapacitor HESS to implement the VSG as different energy storage units are suitable for different control objectives in the VSG. To be specific, the ultracapacitor is used to emulate the inertia of the VSG and cope with high frequency power fluctuations, while the battery is used to emulate the remaining parts of the VSG, e.g. droop control and turbine model, to compensate for relatively long-term power fluctuations with slow dynamics. In this way, the power fluctuations of the battery along with its changing rate can dramatically be reduced. Since the HESS is used to emulate the inertia coefficient, droop control, speed governor and turbine in a VSG model which are all well-known parameters, the controller design of the HESS is very straightforward and does not rely on the conventional low/high pass filters. Experimental results are presented to prove the effectiveness of the proposed HESS-based VSG.

Acknowledgment

This research is supported by the National Research Foundation, Prime Minister's Office, Singapore under the Energy Programme and administrated by the Energy Market Authority (EP Award No. NRF2015EWT-EIRP002-007)

References

[1] J. Rocabert, A. Luna, F. Blaabjerg, and P. Rodriguez, "Control of power converters in AC microgrids," *IEEE Trans. Power Electron.*, vol. 27, DOI 10.1109/TPEL.2012.2199334, no. 11, pp. 4734–4749, Nov. 2012.

[2] P. Kundur, *Power System Stability and Control*. New York, NY, USA: McGraw-Hill, 1994.

[3] F. Blaabjerg, R. Teodorescu, M. Liserre, and A. V. Timbus, "Overview of control and grid synchronization for distributed power generation systems," *IEEE Trans. Ind. Electron.*, vol. 53, DOI 10.1109/TIE.2006.881997, no. 5, pp. 1398–1409, Oct. 2006.

[4] J. Fang, X. Li, X. Yang, and Y. Tang, "An integrated trap-*LCL* filter with reduced current harmonics for grid-connected converters under weak grid conditions," *IEEE Trans. Power Electron.*, vol. 32, DOI 10.1109/TPEL.2017.2651152, no. 11, pp. 8446–8457, Nov. 2017.

[5] J. Driesen and K. Visscher, "Virtual synchronous generators," in *Proc. IEEE Power Energy Soc. Gen. Meeting—Convers. Del. Elect. Energy 21st Century*, DOI 10.1109/PES.2008.4596800, Jul. 2008, pp. 1–3.

[6] H.-P. Beck and R. Hesse, "Virtual synchronous machine," in *Proc. 9th Int. Conf. Elect. Power Qual. Util. (EPQU)*, DOI 10.1109/EPQU.2007.4424220, 2007, pp. 1–6.

[7] Q. Zhong and G. Weiss, "Synchronverters: inverters that mimic synchronous generators," *IEEE Trans. Ind. Electron.*, vol. 58, DOI 10.1109/TIE.2010.2048839, no. 4, pp. 1259–1267, Apr. 2011.

[8] J. Liu, Y. Miura, and T. Ise, "Comparison of dynamic characteristics between virtual synchronous generator and droop control in inverter-based distributed generators," *IEEE Trans. Power Electron.*, vol. 31, DOI 10.1109/TPEL.2015.2465852, no. 5, pp. 3600–3611, May 2016.

[9] J. A. Suul, S. D'Arco, and G. Guidi, "Virtual synchronous machine-based control of a single-phase bi-directional battery charger for providing vehicle-to-grid services," *IEEE Trans. Ind. Appl.*, vol. 52, DOI 10.1109/TIA.2016.2550588, no. 4, pp. 3234–3244, Jul./Aug. 2016.

[10] M. Guan, W. Pan, J. Zhang, Q. Hao, J. Cheng, and X. Zheng, "Synchronous generator emulation control strategy for voltage source converter (VSC) stations," *IEEE Trans. Power Sys.*, vol. 30, DOI 10.1109/TPWRS.2014.2384498, no. 6, pp. 3093–3101, Nov. 2015.

[11] S. M. Lukic, J. Cao, R. C. Bansal, F. Rodriguez, and A. Emadi, "Energy storage systems for automobile applications," *IEEE Trans. Ind. Electron.*, vol. 55, DOI 10.1109/TIE.2008.918390, no. 6, pp. 2258–2267, Jun. 2008.

[12] A. Khaligh and Z. Li, "Battery, ultracapacitor, hybrid energy storage systems for electric, hybrid electric, fuel cell, and plug-in hybrid electric vehicles: state of the art" *IEEE Trans. Veh. Technol.*, vol. 59, DOI 10.1109/TVT.2010.2047877, no. 6, pp. 2806–2814, Jul. 2010.

[13] J. Cao and A. Emadi, "A new battery/ultracapacitor hybrid energy storage system for electric, hybrid, and plug-in hybrid electric vehicles," *IEEE Trans. Power Electron.*, vol. 27, DOI 10.1109/TPEL.2011.2151206, no. 1, pp. 122–132, Jan. 2012.

[14] D. B. W. Abeywardana, B. Hredzak, V. G. Agelidis, and G. D. Demetriades, "Supercapacitor sizing method for energy-controlled filter-based hybrid energy storage system," *IEEE Trans. Power Electron.*, vol. 32, DOI 10.1109/TPEL.2016.2552198, no. 2, pp. 1626–1637, Feb. 2017.

[15] H. Zhou, T. Bhattacharya, D. Tran, T. S. T. Siew, and A. M. Khambadkone, "Composite energy storage system involving battery and ultracapacitor with dynamic energy management in microgrid applications," *IEEE Trans. Power Electron.*, vol. 26, no. 3, DOI 10.1109/TPEL.2010.2095040, pp. 923–930, Mar. 2011.

[16] J. Fang, G. Xiao, X. Yang, and Y. Tang, "Parameter design of a novel series-parallel-resonant *LCL* filter for single-phase half-bridge active power filters," *IEEE Trans. Power Electron.*, vol. 32, no. 1, DOI 10.1109/TPEL.2016.2532961, pp. 200–217, Jan. 2017.

[17] J. Fang, X. Li, and Y. Tang, "Grid-connected power converters with distributed virtual power system inertia," in *Proc. 2017 IEEE Energy Convers. Congr. Expo.* (*ECCE*), in press.

[18] A. Ellis, D. Schoenwald, J. Hawkins, S. Willard, and B. Arellano, "PV output smoothing with energy storage," *2012 38th IEEE Photovoltaic Specialists Conference (PVSC),* DOI 10.1109/PVSC.2012.6317885, 2012, pp. 1523–1528.